supported by the Nederlandse Organisatie voor Wetenschappelijk Onderzoek (NWO), Philips Research and partly supported by the Brite Euram project Tunnel Sense.

Competing interests statement

The authors declare that they have no competing financial interests.

Correspondence and requests for materials should be addressed to Th.R. (e-mail: theoras@sci.kun.nl).

Single-pulse coherently controlled nonlinear Raman spectroscopy and microscopy

Nirit Dudovich, Dan Oron & Yaron Silberberg

Department of Physics of Complex Systems, Weizmann Institute of Science, Rehovot 76100, Israel

Molecular vibrations have oscillation periods that reflect the molecular structure, and are hence being used as a spectroscopic fingerprint for detection and identification. At present, all nonlinear spectroscopy schemes use two or more laser beams to measure such vibrations[1]. The availability of ultrashort (femtosecond) optical pulses with durations shorter than typical molecular vibration periods has enabled the coherent excitation of molecular vibrations using a single pulse[2]. Here we perform single-pulse vibrational spectroscopy on several molecules in the liquid phase, where both the excitation and the readout processes are performed by the same pulse. The main difficulty with single-pulse spectroscopy is that all vibrational levels with energies within the pulse bandwidth are excited. We achieve high spectral resolution, nearly two orders of magnitude better than the pulse bandwidth, by using quantum coherent control techniques. By appropriately modulating the spectral phase of the pulse we are able to exploit the quantum interference between multiple paths to selectively populate a given vibrational level, and to probe this population using the same pulse. This scheme, using a single broadband laser source, is particularly attractive for nonlinear microscopy applications, as we demonstrate by constructing a coherent anti-Stokes Raman (CARS) microscope operating with a single laser beam.

Nonlinear coherent vibrational spectroscopy has evolved during the last two decades as a result of the availability of short pulse sources, the high peak power of which enables detection of the inherently weak nonlinear signals[1,3]. This includes a family of nonlinear processes, typically involving a third-order nonlinearity (that is, three exciting photons) and a Raman active vibrational level. The most commonly used scheme is CARS, the energy level diagram of which is shown in Fig. 1a. In this process, two photons with frequencies ω_1 and ω_2 excite a vibrational level at an energy $\hbar(\omega_1 - \omega_2)$. A third photon at ω_3 interacts with the excited level to emit a signal photon at a frequency $(\omega_1 + \omega_3 - \omega_2)$. Typically, two narrow-band (narrower than the typical linewidth of Raman levels, corresponding to picosecond pulses) beams are used, exciting only Raman levels in resonance with their energy difference (in this case $\omega_1 = \omega_3$). Time-resolved CARS is a variant in which several Raman levels are simultaneously populated by one or two large bandwidth excitation pulses[4] and probed by a delayed probe pulse.

This work demonstrates that the entire CARS process can be incorporated within a single ultrashort pulse. All three photons required for the process are supplied by the same short optical pulse, while quantum coherent control techniques are implemented to restore the high spectral resolution. Furthermore, this technique can overcome the strong nonresonant background which typically accompanies CARS with femtosecond pulses[5].

In coherent control, constructive or destructive interference is induced between the different paths leading to a final quantum state, to manipulate the outcome of a light–matter interaction[6–8]. Control of the simplest nonlinear system, a nonresonant two-photon transition between two levels, was demonstrated by Weiner *et al.*[9] for a Raman transition, and by Meshulach and Silberberg[10] for two-photon absorption. Control over more complicated systems often involves the use of adaptive techniques[11], where the spectral phase is determined by a feedback optimization procedure. This approach has been applied to a variety of systems, such as selective chemical bond breaking[12], high-harmonic generation[13], and controlling the shape of a quantum wavefunction[14]. Spectral resolution enhancement of the standard two-beam CARS excitation scheme by means of coherent control has recently been demonstrated[15,16].

In our experiment we control the population of vibrational energy levels by controlling the spectral phase of a single broadband pulse. The population of a vibrational level at energy Ω_R is proportional to $|\int d\omega E(\omega)E^*(\omega - \Omega_R)|^2$, where $E(\omega) = |E(\omega)|e^{i\Phi(\omega)}$ is the complex spectral amplitude of the applied field. Each level is thus excited by all frequency pairs separated by Ω_R. The interference between the multiple paths leading to the population of the level Ω_R is determined by the relative phase of each contribution $\Phi(\omega) - \Phi(\omega - \Omega_R)$. Constructive interference is achieved when $\Phi(\omega) = \Phi(\omega - \Omega_R)$ for all frequency components of the excitation pulse. For a transform-limited pulse (all frequency components having the same phase) this holds for all values of Ω_R, and so spectral resolution is lost. However, when the spectral phase is modulated periodically with a period Ω, constructive interference is induced for all energy levels where $\Omega_R = N\Omega$ (where N is an integer). We note that a periodic spectral phase is equivalent to splitting the pulse in time domain to several equally spaced pulses, each delayed by $\tau = 2\pi/\Omega$. A coherent population can indeed be built up only if these pulses are separated by an integer number of vibrational periods. By carefully choosing the periodic function it is possible exclusively to populate one Raman level within every frequency octave[9]. In our experiment the excited level population is probed by the excitation pulse itself. All frequency components participate, and the CARS spectrum is therefore similar to the original spectrum, upshifted by the level energy.

The measured signal consists of two components: a nonresonant contribution[1,3], and a resonant Raman contribution. The nonresonant contribution is due to the instantaneous electronic response of

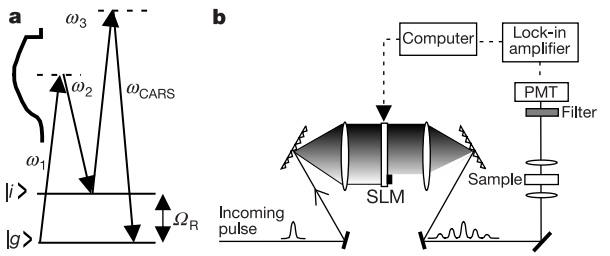

Figure 1 Graphic description of the coherent anti-Stokes Raman (CARS) process and the experimental set-up. **a**, Energy-level scheme of the single-pulse CARS process. The pulse spectrum, blocked on the high-frequency end, has a bandwidth larger than the vibrational energy level. **b**, Diagram of the experimental set-up. The pulse shaper is used to apply the desired phase function by the computer-controlled spatial light modulator (SLM), and to block the high-energy end of the spectrum. The spectral resolution of the shaper is of the order of 0.5 nm. The sample is illuminated by a microscope objective. The CARS signal at higher frequencies, blocked in the incoming pulse, is measured by the photomultiplier tube (PMT). The incoming 20-fs pulses from the Ti:sapphire oscillator are shaped into a pulse train by a periodic phase modulation.

the medium and is determined by the peak intensity of the pulse. For such short pulses it is typically over an order of magnitude stronger than the resonant contribution[5]. Suppression of this background signal is therefore crucial to the observation of any resonant signal. Pulse shaping thus serves two ends, both as a method to excite selectively a vibrational level, and to suppress the nonresonant background, which is maximized by a transform-limited pulse[10], and is weaker for shaped pulses, in which the peak intensity is reduced.

We demonstrate this principle in CARS spectroscopy of several simple molecules in the liquid phase. Our experimental system consists of a mode-locked Ti:sapphire laser emitting 20-fs transform-limited pulses at 80 MHz, a programmable pulse shaper[17], and a photodetector, as shown in Fig. 1b. The Fourier-transform pulse shaper is used both to apply the desired phase to each frequency component of the pulse, and to block the higher frequencies, which may overlap the CARS signal. The sample is illuminated by total bandwidth of 75 nm, equivalent to an energy span of about 1,100 cm^{-1}. After passage through the sample, the excitation pulse is filtered out, and the CARS signal at the high-frequency end is measured. This system is suitable for CARS spectroscopy in the range of about 400–800 cm^{-1}, typical of carbon–halogen bond stretching[1]. The lower limit stems from the technical requirement to filter out the excitation pulse, and the upper limit is due to the total bandwidth.

To measure the Raman spectrum, a sinusoidal spectral phase function is applied to the pulse. The spectrum is obtained by monitoring the total CARS signal, while varying the phase-function periodicity. This, in turn, leads to a nearly sinusoidal variation in the population of any single vibrational level. For a sample with no Raman levels in the measurable range, such as methanol (see Fig. 2a), we merely observe the monotonically decreasing nonresonant signal as the number of oscillation periods is increased. When a sample with a single resonant level, such as CH_2Br_2 (resonant at 577 cm^{-1}, see Fig. 2b) is measured, the signal oscillates. The signal peaks each time the Raman level energy is commensurate with the spectral modulation period. For materials with more than one resonant level, such as $(CH_2Cl)_2$ (resonant at 652 cm^{-1} and 750 cm^{-1}, see Fig. 2c) beats are observed in the signal. The Raman spectrum is obtained by Fourier transformation of the measured signal, as shown in the insets of Fig. 2. The spectral resolution of the Fourier transform operation is better than the pulse bandwidth by a factor of 40 (that is, about 30 cm^{-1}). It is limited by the maximal number of phase modulation periods on the spatial light modulator (SLM), technically determined by the number of pixels on the SLM. Thus, spectral resolution is optimized by use of a simple sinusoidal phase function.

To achieve maximal contrast between the resonant signal and the nonresonant background, however, more complex periodic phase functions should be applied. The contrast is improved by breaking the single pulse to a train containing more pulses, each having a lower energy content, thus reducing its peak intensity. This is achieved by adding higher harmonic orders to the applied phase functions. In Fig. 3 we show how, by using a phase function containing only one additional harmonic, it is possible to attenuate the nonresonant background by nearly two orders of magnitude, while retaining the resonant component. The achieved contrast between the resonant signal and the nonresonant background is thus greatly improved. In fact, using shaped pulses we obtain a predominantly resonant signal, larger by a factor of about four than the nonresonant signal. Such phase functions should be applied when attempting to detect molecules with a known level structure.

Owing to their strong dependence on the local field, nonlinear optical processes are ideal for depth-resolved microscopy. This idea was first implemented for two-photon fluorescence microscopy[18], later used for nonresonant third-harmonic generation processes[19,20], and has been recently extended to CARS[21–23]. CARS microscopy has the potential for studying live biological specimens while gathering three-dimensional information on their molecular structure. Until now, however, CARS microscopes required two or three narrow-band sources. Here, we demonstrate single-pulse spectrally resolved microscopy. The sample consists of a glass capillary plate with 10-μm holes filled with CH_2Br_2 (resonant at 577 cm^{-1}). It was raster-scanned around the focused laser beam using computer-controlled piezoelectric drivers. The image in Fig. 4a was taken with a pulse shape maximizing the relative intensity of the resonant contribution, whereas the image in Fig. 4b was taken with a pulse shape minimizing this intensity. The predominantly resonant signal from the filled holes in Fig. 4a is larger by a factor of four than in Fig. 4b, and the signal from the glass is very similar. Figure 4c shows the difference between Fig. 4a and b, depicting the signal from the 577 cm^{-1} vibrational level of CH_2Br_2. This image appears inverted relative to that obtained using a transform-limited pulse (Fig. 4d), where the glass, having a larger nonresonant signal, appears brighter. The image in Fig. 4c demonstrates the ability of the microscope to spectrally resolve the Raman resonant contribution of a single vibrational level. In a practical system, the difference image could be directly measured by lock-in detection, alternating the phase masks of Fig. 4a and b at a high frequency.

For materials having more than one vibrational level it is possible

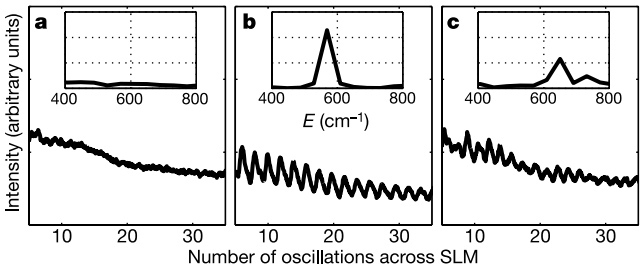

Figure 2 Single-pulse CARS spectroscopy of various organic molecules in the liquid phase. The CARS signal intensity is shown as a function of the number of periods of the sinusoidal phase across the SLM for: **a**, methanol; **b**, CH_2Br_2; **c**, $(CH_2Cl)_2$. The insets show the respective measured Raman spectra, derived by Fourier transformation of the intensity curves. In methanol (**a**), which has no resonance at the measured frequency range, only a monotonically decreasing nonresonant signal is observed. In CH_2Br_2 (**b**), which has a single resonance at $\Omega_R = 577\ cm^{-1}$, the signal peaks periodically, whenever the modulation period is an integer fraction of Ω_R. The Fourier transform operation retrieves the resonance with a resolution that is inversely proportional to the number of observed periods. In $(CH_2Cl)_2$ (**c**), beating between the 652 cm^{-1} and the 750 cm^{-1} levels is observed.

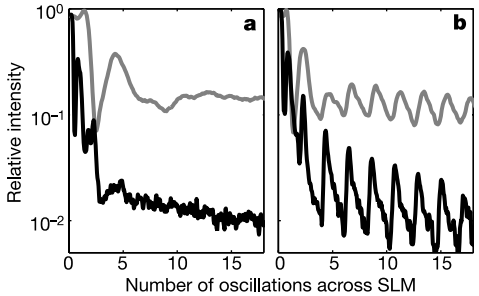

Figure 3 Demonstration of the nonresonant background suppression. The CARS signal intensity is shown as a function of the number of phase oscillation periods across the SLM for both a sinusoidal phase function (grey line) and a phase function containing an additional harmonic component (solid line). The CARS signal is plotted relative to that obtained by a transform-limited pulse (0 phase function oscillations). Results are for: **a**, methanol (nonresonant component only); **b**, CH_3I (a single resonance at 523 cm^{-1}). Suppression of the nonresonant background by nearly two orders of magnitude is achieved (**a**), while the resonant component is almost completely restored. To achieve adequate suppression of the nonresonant background at least several oscillation periods of the phase function across the pulse spectrum are necessary.

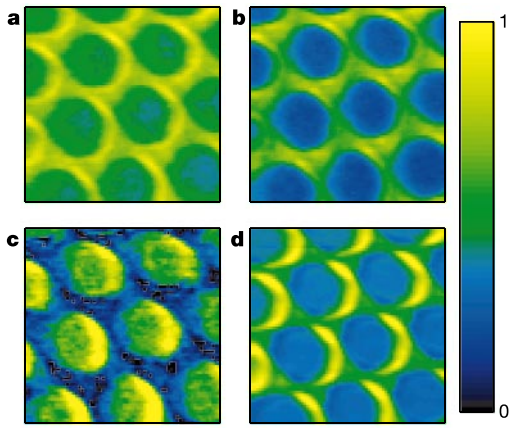

Figure 4 Depth-resolved single-pulse CARS images of a glass capillary plate with 10-μm holes filled with CH_2Br_2 (resonant at 577 cm^{-1}). The average laser power was about 5 mW. **a**, Image obtained using a shaped pulse (similar to the high-contrast one in Fig. 3) maximizing the resonant contribution of the CH_2Br_2 577 cm^{-1} level, while reducing the nonresonant contribution. **b**, Image obtained using a shaped pulse minimizing the resonant contribution of the CH_2Br_2 577 cm^{-1} level. **c**, Difference image, obtained by subtraction of **a** and **b**. This procedure retains only the 577 cm^{-1} resonant component. The image appears inverted relative to an image obtained using a transform-limited pulse (**d**), because a resonant signal appears only in the hole regions containing CH_2Br_2 whereas the nonresonant signal is stronger in the glass. The 45 μm × 45 μm images were obtained using an objective of numerical aperture 0.65, at a rate of 30 ms per pixel. The images are plotted using an arbitrary scale, although in **a** and **b** the same scale is used.

to improve the detection selectivity by tailoring shaped pulses to induce constructive quantum interference of these levels. A simple example is the shape used to obtain peaks in the beat signal of Fig. 2c, where the resonant contributions of two levels of $(CH_2Cl)_2$ constructively interfere.

Our experiment shows how single-pulse vibrational microspectroscopy can be readily achieved by using coherent control techniques. By tailoring the spectral phase of an ultrashort pulse, we are able to control the interference between the various spectral components of the pulse, leading to selective population of given vibrational energy levels. By applying this principle, we have demonstrated a robust method for high-resolution spectroscopy, nearly two orders of magnitude greater than the spectral bandwidth, in the vibrational energy range 400–800 cm^{-1}. This method is easily extendable to the fingerprint region (1,000–1,500 cm^{-1}) by using slightly shorter pulses, available in commercial systems today. Single-pulse CARS is particularly suitable for nonlinear microscopy. In contrast to conventional nonlinear CARS microscopy, which requires two synchronized tunable sources, single-pulse CARS requires only a single ultrashort laser that does not need to be tuned. The spectral measurements are performed with an electronically controlled SLM. Moreover, it can be easily combined with other nonlinear microscopic methods such as multiphoton fluorescence and third-harmonic generation using the same microscope set-up. The concept of performing a nonlinear optical interaction with matter in a single coherently controlled pulse offers a promising alternative to standard multiple-pulse nonlinear systems in use today. We believe that combined with present-day sources, covering most of the optical spectrum in a single pulse, this concept will have a significant impact on nonlinear spectroscopy and microscopy applications. □

Received 8 January; accepted 19 June 2002; doi:10.1038/nature00933.

1. Kiefer, W. in *Infrared and Raman Spectroscopy* (ed. Schrader, B.) 162–188 (VCH, Weinheim, 1995).
2. Yan, Y. X., Cheng, L. T. & Nelson, K. A. in *Advances in Spectroscopy* (eds Clark, R. J. H. & Hester, R. E.) Vol. 16, 299–355 (Wiley, Chichester, 1988).
3. Levenson, M. D. *Introduction to Nonlinear Laser Spectroscopy* (Academic, New York, 1982).
4. Leonhardt, R., Holzapfel, W., Zinth, W. & Kaiser, W. Terahertz quantum beats in molecular liquids. *Chem. Phys. Lett.* **133,** 373–377 (1986).
5. Cheng, J., Volkmer, A., Book, L. D. & Xie, X. S. An epi-detected coherent anti-Stokes Raman scattering (E-CARS) microscope with high spectral resolution and high sensitivity. *J. Phys. Chem. B* **105,** 1277–1280 (2001).
6. Tannor, D. J. & Rice, S. A. Control of selectivity of chemical reaction via control of wavepacket evolution. *J. Chem. Phys.* **83,** 5013–5018 (1985).
7. Shapiro, M. & Brumer, P. Laser control of product quantum state populations in unimolecular reactions. *J. Chem. Phys.* **84,** 4103–4104 (1986).
8. Warren, W. S., Rabitz, H. & Dahleh, M. Coherent control of quantum dynamics: the dream is alive. *Science* **259,** 1581–1589 (1993).
9. Weiner, A. M., Leaird, D. E., Wiederrecht, G. P. & Nelson, K. A. Femtosecond pulse sequences used for optical manipulation of molecular motion. *Science* **247,** 1317–1319 (1990).
10. Meshulach, D. & Silberberg, Y. Coherent quantum control of two-photon transitions by a femtosecond laser pulse. *Nature* **396,** 239–242 (1998).
11. Judson, S. R. & Rabitz, H. Teaching lasers to control molecules. *Phys. Rev. Lett.* **68,** 1500–1503 (1992).
12. Assion, A. *et al.* Control of chemical reaction by feedback-optimized phase-shaped femtosecond laser pulses. *Science* **282,** 919–922 (1998).
13. Bartels, R. *et al.* Shaped pulse optimization of coherent emission of high-harmonic soft X-rays. *Nature* **406,** 164–166 (2000).
14. Weinacht, T. C., Ahn, J. & Bucksbaum, P. H. Controlling the shape of a quantum wavefunction. *Nature* **397,** 233–235 (1999).
15. Oron, D., Dudovich, N., Yelin, D. & Silberberg, Y. Quantum control of coherent anti-Stokes Raman processes. *Phys. Rev. A* **65,** 043408-1–043408-4 (2002).
16. Oron, D., Dudovich, N., Yelin, D. & Silberberg, Y. Narrow band coherent anti-Stokes Raman signals from broadband pulses. *Phys. Rev. Lett.* **88,** 063004-1–063004-4 (2002).
17. Weiner, A. M. Femtosecond pulse shaping using spatial light modulators. *Rev. Sci. Instrum.* **71,** 1929–1960 (2000).
18. Denk, W., Strickler, J. H. & Webb, W. W. Two-photon laser scanning fluorescence microscopy. *Science* **248,** 73–76 (1990).
19. Barad, Y., Eisenberg, H., Horowitz, M. & Silberberg, Y. Nonlinear scanning laser microscopy by third harmonic generation. *Appl. Phys. Lett.* **70,** 922–924 (1997).
20. Muller, M., Squier, J., Wilson, K. R. & Brakenhoff, G. J. 3D microscopy of transparent objects using third harmonic generation. *J. Microsc.* **191,** 266–274 (1998).
21. Zumbusch, A., Holtom, G. R. & Xie, X. S. Three-dimensional vibrational imaging by coherent anti-Stokes Raman scattering. *Phys. Rev. Lett.* **82,** 4142–4145 (1999).
22. Potma, E. O., de Boeij, W. P., van Haastert, P. J. M. & Wiersma, D. A. Real-time visualization of intracellular hydrodynamics in single living cells. *Proc. Natl Acad. Sci. USA* **98,** 1577–1582 (2001).
23. Muller, M., Squier, J., de Lange, C. A. & Brakenhoff, G. J. CARS microscopy with folded BoxCARS phasematching. *J. Microsc.* **197,** 150–158 (2000).

Acknowledgements

We thank D. Mandelik for his aid in preparing the microscope samples. Financial support by the Israeli Science Foundation and by the Bundesministerium fur Bildung und Forschung is gratefully acknowledged.

Competing interests statement

The authors declare that they have no competing financial interests.

Correspondence and requests for materials should be addressed to Y.S. (e-mail: yaron.silberberg@weizmann.ac.il).

A large-cavity zeolite with wide pore windows and potential as an oil refining catalyst

Avelino Corma*, María J. Díaz-Cabañas*, Joaquín Martínez-Triguero*, Fernando Rey* & Jordi Rius†

** Instituto de Tecnología Química, UPV-CSIC, Universidad Politécnica de Valencia, Avda. de los Naranjos s/n, 46022 Valencia, Spain*
† Institut de Ciència de Materials de Barcelona (CSIC), Campus de la UAB, 08193-Bellaterra, Catalunya, Spain

Crude oil is an important feedstock for the petrochemical industry and the dominant energy source driving the world economy, but known oil reserves will cover demand for no more than 50 years at the current rate of consumption[1]. This situation calls for more efficient strategies for converting crude oil into fuel and petrochemical products. At present, more than 40% of oil conversion is achieved using catalysts based on